

Wigner crystal of a screened-Coulomb-interaction colloidal system in two dimensions

F. M. Peeters and Xiaoguang Wu

Departement Natuurkunde, Universitaire Instelling Antwerpen, Universiteitsplein 1, B-2610 Antwerpen (Wilrijk), Belgium

(Received 20 October 1986)

The phase diagram of a two-dimensional system consisting of colloids is investigated within the Kosterlitz-Thouless-Halperin-Nelson-Young theory of dislocation-mediated two-dimensional melting. We also present results for the interaction energy, the phonon spectrum, and the longitudinal and transverse sound velocity for different values of the screening length.

I. INTRODUCTION

It is well established (see, e.g., Refs. 1 and 2 for recent reviews) that a system of colloidal spheres (e.g., of polystyrene spheres) submerged in aqueous suspensions can exhibit transitions from an ordered to a disordered state (liquid). The crystal-ordering forces in this three-dimensional (3D) system have been shown³ to be electrostatic, which are similar to those in the two-dimensional (2D) system of electrons on a liquid-helium surface. The latter have been found⁴ to crystallize into a Wigner lattice.⁵ The main advantage of the system of colloids in comparison to the system of electrons on helium is that one is directly able to see the motion of the spheres through a microscope. Thus one is able to detect optically (without perturbing the system) the state of the system.

Up to now the main attention of theorists and experimentalists was focused on the study of 3D systems of colloids. Only a few recent⁶⁻⁸ experiments were directed towards the observation of the effect of spatial confinement of the colloids on their collective properties. For example, in Refs. 7 and 8 one was able to induce a continuous transition between 2D and 3D behavior by the use of a wedge.

In the present paper we study the 2D behavior of colloids. Pieranski⁶ studied experimentally a 2D colloidal crystal formed at a water-air interface. The interaction between those colloids was found to be a dipole repulsion which is a consequence of the asymmetry in the charge distribution due to the specific experimental configuration. The system was studied theoretically in Ref. 9.

The 2D system we envisage is depicted in Fig. 1. The colloids are confined between two solid surfaces which are, on the colloidal scale, perfectly rigid, smooth, and parallel. The distance between the two solid surfaces (d) can be varied continuously. The colloidal particles are taken as identical spheres with a radius a typically between 100 and 10 000 Å. When dissolved in, for example, water (dielectric constant $\epsilon=80$), endgroups dissociate from the colloid which leads to a large electrostatic charge Z per colloidal particle. The dissociated endgroups are single molecules and are considered as providing a background of continuum charges. These counterions will screen the direct Coulomb interaction between the colloids. A simple calculation shows that the image charges induced in the two confining plates have the same sign and are of the same order of magnitude as the charge of

the colloidal particles itself because of the relatively large dielectric constant of the medium (i.e., $\epsilon=80$). These image charges will induce a potential in the direction perpendicular to the plates which will force the colloids in the middle between the two plates.

The interaction between the polyballs is quite complicated. But it has been claimed^{2,10} that a simple screened Coulomb interaction may still be used to describe the long-range interaction if the charge Z is normalized to Z^* . We take for the electrostatic interaction between two colloidal particles

$$U(r) = \frac{(Z_\lambda e)^2}{\epsilon} \frac{e^{-r/\lambda}}{r}, \tag{1}$$

with λ the screening length, ϵ the dielectric constant of the medium (we will take $\epsilon=80$), and $Z_\lambda = Z^* f(a/\lambda)$, where Z^* is the normalized charge and $f(x)$ is a form factor which describes the effect of the nonzero radius a of the colloidal particles. We will follow Ref. 11 and take $f(x) = \sinh(x)/x$. Others^{2,12} have taken a different form $f^*(x) = e^x/(1+x)$ which has essentially the same functional behavior as the one of Sogami. For $x \rightarrow 0$ they are equal but with increasing x , $f^*(x)/f(x)$ increases to a factor of 2 in the limit $x \rightarrow \infty$.

The screening of the Coulombic interaction is taken as three dimensional because the counterions are free to move in the z direction (which is taken perpendicular to the 2D colloidal layer) but bounded by the two plates. The screening length λ is given by the usual expression

$$\lambda^2 = \frac{\epsilon k_B T}{4\pi e^2 n_{3D}}, \tag{2}$$

with n_{3D} the three-dimensional charge density of the

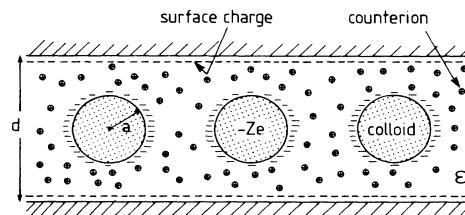


FIG. 1. Experimental configuration for a 2D system of colloids.

counterions and k_B the Boltzmann's constant. The counterions are provided by the colloidal particles and lead to a charge density Z^*n_{2D}/d , because they are distributed over the slab with thickness d . It is possible that the surfaces of the confining plates are charged when they are brought in contact with water. This leads to a plate-surface charge density⁸ n_s ($\sim 2.5 \times 10^{14} \text{ cm}^{-2}$ for glass plates) and consequently it gives a contribution of $2n_s/d$ to the counterion charge density. Thus $n_{3D} = (2n_s + Z^*n_{2D})/d$, where we assumed that the plate surface is charged negatively as is the case for glass plates.⁸ It is interesting to see that on the basis of local charge neutrality the screening length in the system can be varied continuously by changing the distance between the two plates. To give an idea of the order of magnitude, we have plotted in Fig. 2 the screening length λ versus the distance between the two plates for charged (we took $n_s = 2.5 \times 10^{14} \text{ cm}^{-2}$) and neutral plates. The temperature was taken equal to 300 K.

It is interesting to note that a similar situation was encountered for the electrons on a thin liquid-helium-film system¹³ where the reduction of the thickness of the liquid-helium film leads to a screening of the direct Coulomb interaction between the electrons. In the present system the plates have to move closer to each other to increase the screening which should be compared with a thinning down of the helium film in the case of electrons on helium.

In order to investigate the phase diagram we will make use of the now generally accepted picture of classical 2D melting by the unbinding of pairs of defects as first suggested by Kosterlitz and Thouless¹⁴ (KT) and later elab-

orated on by Halperin and Nelson¹⁵ (HN) and Young (Y).¹⁶ This theory was very successfully applied¹⁷ to the classical system of electrons on helium. It predicted correctly the phase diagram.

The KTHNY theory describes melting of a classical 2D solid irrespective of the interaction between the particles and can thus also be applied to the present system. The aim of the present paper is to apply this theory to the system of particles which interact with a screened Coulomb potential. This system may be considered as a *model system* for melting of a 2D system of colloids. The KTHNY theory states that at the melting transition¹⁵

$$\frac{16\pi k_B T}{b^2} = \frac{4\mu_0(\mu_0 + \lambda_0)}{2\mu_0 + \lambda_0}, \quad (3)$$

where μ_0, λ_0 are the Lamé coefficients of the 2D solid and b is the lattice constant.

The present paper is organized as follows. In Sec. II we calculate the interaction energy of a triangular lattice and of a square lattice. We find that the triangular lattice has the lowest energy for all values of the screening length. The phonon spectrum for the triangular lattice is calculated along the boundary of the irreducible element of the Brillouin zone. The longitudinal (C_l) and the transverse (C_t) sound velocity are calculated in Sec. III which then will be inserted into Eq. (3) in order to obtain the phase diagram. Our conclusions are presented in Sec. IV.

II. INTERACTION ENERGY AND PHONON SPECTRUM

Because the system is classical it is possible to separate the kinetic energy and the potential energy. For the considered temperature (i.e., $T = 300 \text{ K}$) the kinetic energy equals $k_B T$. The interaction energy of one colloidal particle with all the other particles is given by

$$E_l^{(c)} = \sum_{l (\neq 0)} U(\mathbf{R}(l)), \quad (4)$$

where $\mathbf{R}(l)$ is the lattice position of the particle at site l (the colloidal system is considered in the solid phase). The interaction two-particle energy $U(r)$ is given by Eq. (1). The lattice sum runs over all possible lattice positions (l) except the origin. Because of the exponential screening the sum in Eq. (4) converges relatively fast and it is not necessary to apply the Ewald summation technique as in the case for long-range potentials^{13,18} like, for example, the pure Coulomb potential.

We considered two different lattices: (i) a square lattice with unit vectors $(b, 0)$ and $(0, b)$ and (ii) a triangular lattice with translation vectors $(b, 0)$ and $(b/2, b\sqrt{3}/2)$. It is convenient to use $E_0 = (Z_\lambda e)^2 / \epsilon b$ as the unit of energy and the interaction energy then depends only on the variable a_s / λ where $a_s = 1 / \sqrt{n_{2D}}$ and $b / a_s = 1$ for the square lattice and

$$b / a_s = (2/\sqrt{3})^{1/2} = 1.074 569 9$$

for the triangular lattice.

Note that we have still to add the interaction energy of the particle with the background ($E_l^{(b)}$), which in the present case is taken as a uniform continuum of coun-

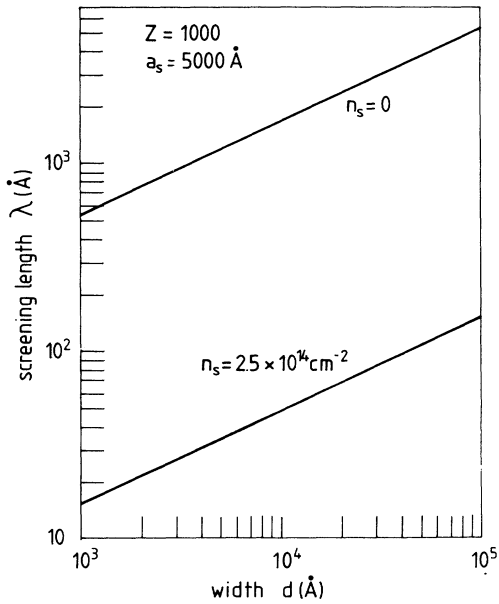


FIG. 2. The screening length λ (in Å) vs the width of the slab d (in Å) for a 2D system of colloids with average separation $a_s = 5000 \text{ \AA}$ and effective charge $Z^* = 1000$ at $T = 300 \text{ K}$, in the case with ($n_s = 2.5 \times 10^{14} \text{ cm}^{-2}$) and without ($n_s = 0$) surface-plate charges.

terion charges. The counterions are distributed over the slab with width d and consequently $E_I^{(b)}$ will be a function of d . This d dependence is not crucial in determining which lattice type has the lowest energy. Therefore when we present numerical results we will consider the background charge as being distributed in the 2D plane of the colloidal particles. This choice has the additional advantage that we will be able to reobtain some known results. Namely, the interparticle potential under consideration [Eq. (1)] contains the Coulomb potential as a special case, namely, $\lambda \rightarrow \infty$. In this limit the known results¹⁸ for the interaction energy should be reobtained.

The interaction with the neutralizing background gives a negative contribution

$$E_I^{(b)}/E_0 = -\frac{2\pi b}{a_s} \frac{1}{(a_s/\lambda)}$$

The resulting interaction energy $E_I = E_I^{(c)} + E_I^{(b)}$ is shown in Fig. 3 as a function of a_s/λ for the triangular and the square lattice. We found that the triangular lattice gives the lowest interaction energy and is thus the most stable solid phase for all values of the screening length. This is in contrast with the 3D system of colloids where it was found^{2,12,19,20} that a structural phase transition takes place from an fcc to a bcc lattice with increasing screening length λ .

In the zero screening limit the results for the 2D Coulomb solid are reobtained,¹⁸ i.e., $E_I/E_0 = -4.213425$ for the triangular lattice and -3.900265 for the square lattice. In Refs. 13 and 18 the interaction energy was referred to $E_0 b/a_s$ and if we make that conversion the present results coincide with those of Refs. 13 and 18. In the large screening limit, i.e., $a_s/\lambda \rightarrow \infty$, we found $E_I/E_0 = -6.751722/(a_s/\lambda)$ for the triangular lattice and $-6.283185/(a_s/\lambda)$ for the square lattice.

Next we will calculate the phonon spectrum of the 2D colloidal solid. The frequency of the two normal vibrational modes are given by

$$\omega_{\pm}^2(\mathbf{q}) = \frac{1}{2}(C_{xx}(\mathbf{q}) + C_{yy}(\mathbf{q}) \pm \{ [C_{xx}(\mathbf{q}) - C_{yy}(\mathbf{q})]^2 + 4C_{xy}^2(\mathbf{q}) \}^{1/2}), \quad (5)$$

with the dynamical matrix

$$C_{ij}(\mathbf{q}) = -\frac{e^2}{m} [S_{ij}(\mathbf{q}) - S_{ij}(0)] \quad (6a)$$

and the matrix

$$S_{ij}(\mathbf{q}) = \frac{1}{e_2} \frac{\partial^2}{\partial R_i \partial R_j} \sum_{l(\neq 0)} V(\mathbf{R} - \mathbf{R}(l)) e^{-i\mathbf{q} \cdot \mathbf{R}(l)}. \quad (6b)$$

The unit of frequency is taken to be ω_0 with

$$\omega_0^2 = \frac{(Z\lambda e)^2}{\epsilon} \frac{1}{mb^3}$$

and the unit of wave vector is $1/b$. As seen above, the triangular lattice has the lowest energy. Therefore we will only give the phonon spectrum for this type of lattice. Furthermore, we found that the square lattice exhibits pure imaginary transverse normal mode frequencies in certain directions in q space which imply that such a lattice is unstable. This result is a generalization of a similar observation made by Bonsall and Maradudin¹⁸ for the 2D Coulomb lattice.

The phonon spectrum is shown in Fig. 4 along the boundary of the irreducible element of the first Brillouin zone for different values of the parameter a_s/λ . The $a_s/\lambda = 0$ result is identical to the 2D Coulomb result of Bonsall and Maradudin.¹⁸ From Fig. 4 it is apparent that with increasing screening the phonon modes soften. Further the longitudinal mode for a long-range Coulomb solid has a square-root dependence on the wave vector for small wave vectors, i.e., $\omega_l \sim \sqrt{q}$, while for the screened system the longitudinal mode becomes acoustical. This is similar to the system of 2D electrons on a thin liquid-helium film¹³ where the interparticle interaction is screened by the substrate which supports the liquid-helium film. Also note that the acoustical branch has a *superlinear* behavior, as was first noted by Platzman and Fukuyama.²¹ This superlinear behavior becomes less pronounced with increasing screening.

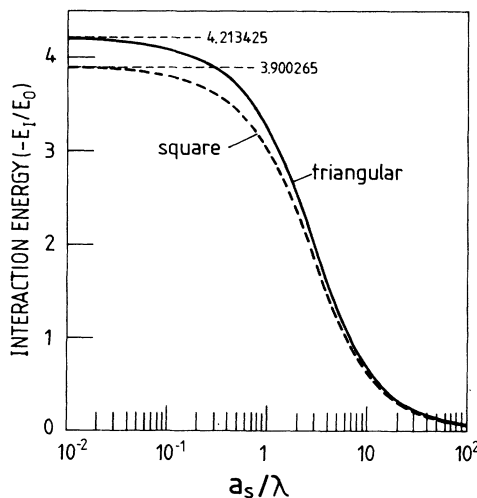


FIG. 3. The interaction energy for the ideal 2D configuration (i.e., $d=0$) vs a_s/λ for a triangular and a square lattice.

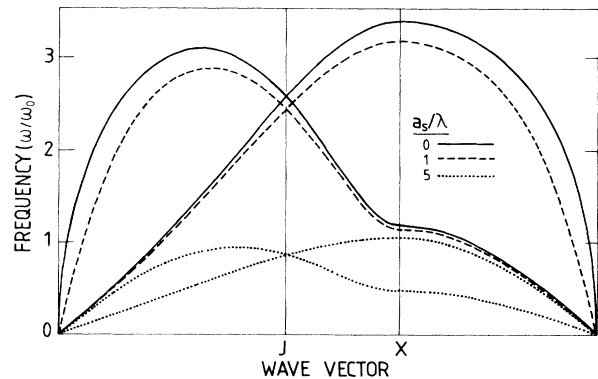


FIG. 4. The phonon spectrum for the triangular lattice along the irreducible element of the first Brillouin zone for a Coulomb system (i.e., $a_s/\lambda=0$) and for two different values of the screening length, namely, $\lambda=a_s$ and $\lambda=a_s/5$.

III. PHASE DIAGRAM

The 2D theory for *dislocation-mediated melting* expresses the phase diagram in terms of the two Lamé coefficients [see Eq. (3)]. These coefficients are related to the longitudinal (C_l) and the transverse (C_t) sound velocities in the following way (see, e.g., Ref. 22),

$$\begin{aligned}\mu_0 &= \rho C_t^2, \\ \lambda_0 &= \rho(C_l^2 - 2C_t^2),\end{aligned}\quad (7)$$

where μ_0 is also dubbed the *shear modulus* and $\rho = mn_{2D}$ is the mass density. It is interesting to note that the shear modulus is a quantity which can be measured experimentally (for such an experiment we refer to, e.g., Refs. 23, 24, 25, and 26).

The sound velocities are defined as $\omega = Cq$ for $q \rightarrow 0$. They are shown in Fig. 5 as function of the parameter a_s/λ . The unit of velocity is

$$C_0 = \omega_0 b = \left(\frac{(Z_\lambda e)^2}{\epsilon} \frac{1}{mb} \right)^{1/2}.$$

The velocities are decreasing functions with increasing a_s/λ . In the limit of zero screening (i.e., $a_s/\lambda \rightarrow 0$) we find

$$\begin{aligned}C_l/C_0 &= 0.51317 - 0.0226(a_s/\lambda)^2, \\ C_t/C_0 &= 2.585/(a_s/\lambda)^{1/2}.\end{aligned}$$

Note that at $a_s/\lambda = 0$ the known results are found. In the opposite limit of large screening ($a_s/\lambda \rightarrow \infty$) we found that the sound velocities C_l and C_t go to zero.

When we insert the results for the sound velocities into Eq. (3), the phase diagram results. In the above units this is given by

$$b = \frac{1}{2\pi\sqrt{3}} \frac{(Z_\lambda e)^2}{\epsilon k_B T} F \left(\frac{a_s}{\lambda} \right), \quad (8)$$

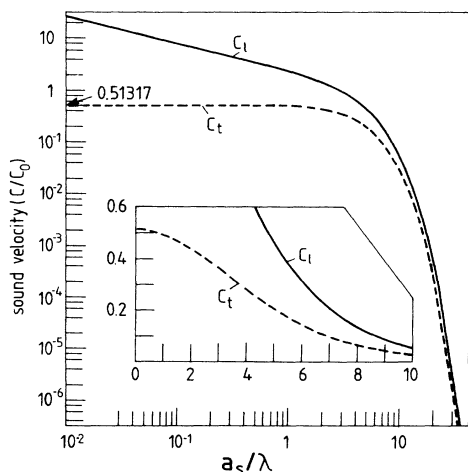


FIG. 5. The longitudinal (C_l) and transverse (C_t) sound velocity as function of a_s/λ .

where

$$F \left(\frac{a_s}{\lambda} \right) = \left(\frac{C_l}{C_0} \right)^2 \left[1 - \left(\frac{C_t}{C_l} \right)^2 \right]. \quad (9)$$

Equation (8) is a nonlinear equation which has to be solved numerically. The result is shown in Figs. 6 and 7 for a fixed $T = 300$ K and $\epsilon = 80$. In the colloidal system the phase diagram is usually studied at constant temperature. The reason is that temperature has a not-so-well-known influence on several parameters in the system, such as Z^* and ϵ . Therefore one generally chooses the screening length as the parameter which drives the system through the phase transition. Thus roughly we can say that the potential energy is changed instead of the kinetic energy, as in the electron on helium system, when the system transforms from the solid to the liquid phase.

In Fig. 6 the phase diagram is given for a fixed sphere radius $a = 250$ Å and for different values of the effective particle charge. In Fig. 7 the particle charge is kept constant at $Z^* = 1000$ and the influence of the radius of the particles on the phase diagram is investigated.

From these two figures we can conclude the following: (i) The curve at which the phase transition takes place never enters the forbidden region. The forbidden region is bounded by the condition at which the spheres are touching each other (i.e., the close packing configuration): $a_s/a = (2\sqrt{3})^{1/2} = 1.8612097$ (the particles cannot penetrate each other). It is interesting to observe that the present theory is aware of this condition. (ii) At a fixed particle density the solid phase is more stable with increasing effective charge Z^* (see Fig. 6). (iii) For a fixed screening length one needs larger sphere separations to melt the system if the spheres are larger (see Fig. 7). Thus bigger spheres will much more easily form a solid. This is

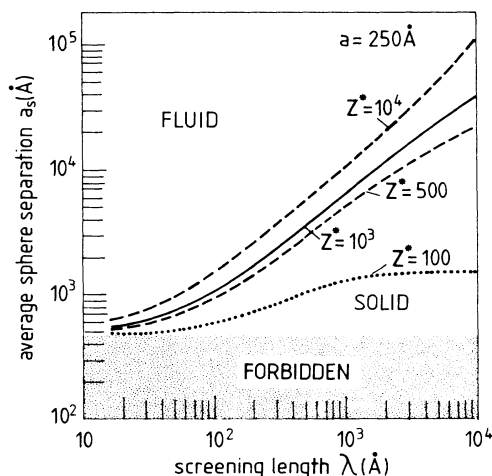


FIG. 6. The phase diagram for a 2D system of colloids with sphere radius $a = 250$ Å and different values of the sphere effective charge Z^* . The region labeled "forbidden" corresponds to the unphysical situation where the colloids would overlap.

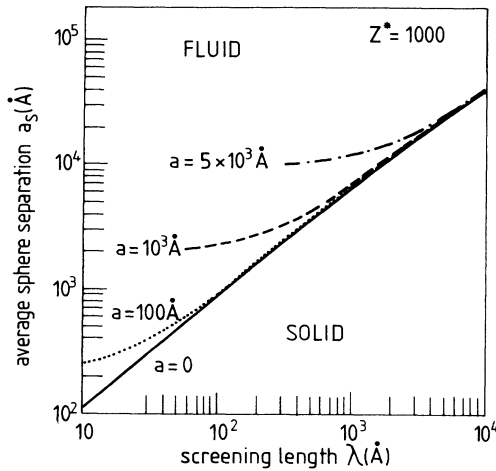


FIG. 7. The same as Fig. 6 but now for a fixed-sphere effective charge $Z^* = 1000$ and for different values of the sphere radius a .

true except for large values of the screening length where this dependence on the sphere radius a disappears.

IV. CONCLUSIONS

We have studied the solid-liquid phase diagram of a 2D system of colloids confined between two plates. As far as we know this is the first analysis of such a system in terms of the dislocation-mediated melting theory of 2D solids of Kosterlitz-Thouless-Halperin-Nelson-Young. The Lamé coefficients are calculated within the harmonic approximation and thermal fluctuations are neglected. The inclusion of thermal effects will lead to corrections to the Lamé coefficients which will change the position of the phase transition *quantitatively*. Nevertheless we expect that the present theoretical analysis will give a good qualitative picture of the phase diagram for a 2D colloidal system. For example, we believe that the general trends as far as the *qualitative* dependence on λ , a , and Z^* is correctly described by the present rather simple approach. At present we feel that there are several parameters which are not well understood like, for example, the applicability of the screened Coulomb potential for the present system (see, e.g., Refs. 25 and 26) and the importance of hydrodynamic forces which have been shown^{25,26} to overdamp the phonon modes in a 3D colloidal system. Therefore we think that before we attempt a more quantitative accurate calculation it will be necessary to investigate the form of the potential and, for example, the charge renormalization in the present 2D system. This will be left for future work.

In many works in connection with one-component plasmas (OCP) a plasma parameter is defined which characterizes the classical OCP completely. This parameter is given by

$$\Gamma = \frac{(Ze)^2}{\epsilon k_B T r_s}, \quad (10)$$

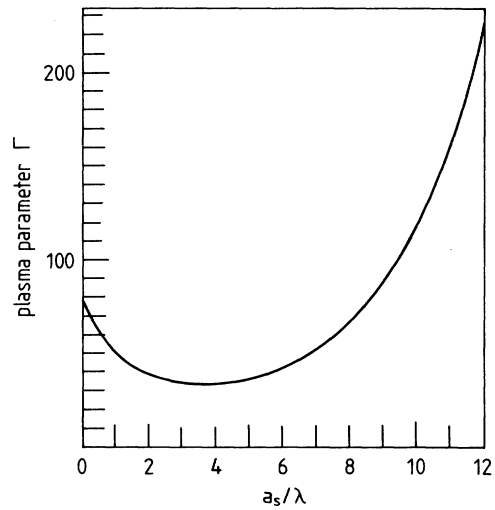


FIG. 8. Value of the plasma parameter Γ for which a solid-liquid phase transition takes place for a 2D screened Coulomb system.

where in 2D $r_s = 1/\sqrt{\pi n_{2D}} = a_s/\sqrt{\pi}$ and which in fact is the ratio of the average potential energy to the average kinetic energy. For the present system with screened Coulomb interactions this becomes

$$\Gamma = \frac{(Z_\lambda e)^2}{\epsilon k_B T r_s} e^{-r_s/\lambda}. \quad (11)$$

From the present theory we can calculate the value of Γ at the phase-transition point. The result is shown in Fig. 8 as function of a_s/λ . In the limit of no screening we found $\Gamma = 78.71$ as obtained earlier in Ref. 27. The experimental result for a Coulomb system of electrons on helium is $\Gamma \sim 125$ which can be explained¹⁷ by the KTHNY theory if one incorporates the temperature dependence of the shear modulus arising from the phonon-phonon interaction and the polarizability of dislocation pairs.

In conclusion we state that the 2D colloidal system provides a nice experimentally realizable system at which 2D melting can be studied. Several experimental variable parameters are available (e.g., the thickness d of the 2D slab, the radius of the spheres a , the charge of the spheres Z^* , the counterion content, etc.) which will influence the interparticle interaction (e.g., via the screening length λ) in one or another way.

The KTHNY theory allows for the possibility of the existence of a *hexatic phase*. Recent computer simulations²⁸ seem to confirm the existence of such a phase. In this phase the system has lost its translational order but there is still *quasi-long-range* orientational order. In the case of the "electrons on helium" system no such hexatic phase has been demonstrated. The difficulty there has an experimental origin: how to discriminate experimentally between a liquid phase and a hexatic phase? In the present system under study the different colloidal particles can be seen through a microscope and this should al-

low one to observe directly such a hexatic phase.²⁹ In the present paper we concentrated on the solid-liquid transition which is defined as the transition where translational order disappears. In the phase diagrams shown in Figs. 6 and 7 the hexatic phase would be located along the phase line on the liquid side. Then there should be another phase line for the transition from the hexatic to the isotropic liquid phase.

ACKNOWLEDGMENTS

One of the authors (F.M.P.) acknowledges financial support from the Belgian National Fund for Scientific Research. X. Wu wishes to thank the International Culture Co-operation of Belgium for financial support. It is a pleasure to thank C. C. Grimes and in particular C. A. Murray for encouragement and helpful discussions during the course of this work.

-
- ¹P. Pieranski, *Contemp. Phys.* **24**, 25 (1983).
²D. Hone, *J. Phys. (Paris), Colloq.* **46**, C3-21 (1985).
³R. Williams and R. S. Crandall, *Phys. Rev. Lett.* **48A**, 224 (1974); R. Williams, R. S. Crandall, and P. J. Wojtowicz, *Phys. Rev. Lett.* **37**, 348 (1976).
⁴C. C. Grimes and G. Adams, *Phys. Rev. Lett.* **42**, 795 (1979).
⁵E. Wigner, *Trans. Faraday Soc.* **34**, 678 (1938).
⁶P. Pieranski, *Phys. Rev. Lett.* **45**, 569 (1980).
⁷P. Pieranski, L. Strzlecki, and B. Pansu, *Phys. Rev. Lett.* **50**, 900 (1983).
⁸D. M. Van Winkle and C. A. Murray, *Phys. Rev. A* **34**, 562 (1986).
⁹R. K. Kalia and P. Vashishta, *J. Phys. C* **14**, L643 (1981).
¹⁰S. Alexander, P. M. Chaikin, P. Grant, G. J. Morales, P. Pincus, and D. Hone, *J. Chem. Phys.* **80**, 5776 (1984).
¹¹I. Sogami, *Phys. Lett. A* **96**, 199 (1983); I. Sogami and N. Ise, *J. Chem. Phys.* **81**, 6320 (1984).
¹²W. H. Shih and D. Stroud, *J. Chem. Phys.* **79**, 6254 (1983).
¹³F. M. Peeters and P. M. Platzman, *Phys. Rev. Lett.* **50**, 2021 (1983); F. M. Peeters, *Phys. Rev. B* **20**, 159 (1984).
¹⁴M. Kosterlitz and D. Thouless, *J. Phys. C* **6**, 1181 (1973).
¹⁵B. Halperin and D. Nelson, *Phys. Rev. Lett.* **41**, 121 (1978); **41**, 519(E) (1978); D. Nelson and B. Halperin, *Phys. Rev. B* **19**, 2457 (1979).
¹⁶P. Young, *Phys. Rev. B* **19**, 1855 (1979).
¹⁷R. H. Morf, *Phys. Rev. Lett.* **43**, 931 (1979).
¹⁸L. Bonsall and A. A. Maradudin, *Phys. Rev. B* **15**, 1959 (1977).
¹⁹H. M. Lindsay and P. M. Chaikin, *J. Chem. Phys.* **76**, 3774 (1982).
²⁰J. M. e Silvo and B. J. Mokross, *Solid State Commun.* **33**, 493 (1980); *Phys. Rev. B* **21**, 2972 (1980).
²¹P. M. Platzman and H. Fukuyama, *Phys. Rev. B* **10**, 3150 (1974).
²²L. D. Landau and E. M. Lifshitz, *Theory of Elasticity* (Pergamon, London, 1959), p. 98.
²³E. Dubois-Violette, P. Pieranski, F. Rothen, and L. Strzlecki, *J. Phys. (Paris)* **41**, 369 (1980).
²⁴B. J. Ackerson and N. A. Clark, *Phys. Rev. Lett.* **46**, 123 (1981).
²⁵F. Grüner and W. P. Lehmann, *J. Phys. A* **15**, 2847 (1982).
²⁶A. J. Hurd, N. A. Clark, R. C. Mockler, and W. J. O'Sullivan, *Phys. Rev. A* **26**, 2869 (1982).
²⁷D. J. Thouless, *J. Phys. C* **11**, L189 (1978).
²⁸D. Frenkel and J. P. McTague, *Phys. Rev. Lett.* **42**, 1632 (1979); J. Tobochnik and G. V. Chester, in *Ordering in Two Dimensions*, edited by Sinha (North-Holland, Amsterdam, 1980), p. 339; V. M. Bedanov, G. V. Gadiyak, and Yu. E. Lozovik, *Zh. Eksp. Teor. Fiz.* **88**, 1622 (1985) [*Sov. Phys.—JETP* **61**, (1985)].
²⁹Recently C. A. Murray has observed a hexatic phase for a 2D system of colloids [C. A. Murray and D. H. Van Winkle, *Phys. Rev. Lett.* (to be published)].